Pattern Recognition Letters 31 (2010) 1751–1758

Contents lists available at ScienceDirect

Pattern Recognition Letters

journal homepage: www.elsevier.com/locate/patrec

AntShrink: Ant colony optimization for image shrinkage

Jing Tian [a], Weiyu Yu [b,*], Lihong Ma [c]

[a] BLK 523, Jelapang Road, Singapore 670523, Singapore
[b] School of Electronic and Information Engineering, South China University of Technology, Guangzhou 510641, PR China
[c] Guangdong Key Lab. of Wireless Network and Terminal, School of Electronic and Information Engineering, South China University of Technology, Guangzhou 510641, China

ARTICLE INFO

Article history:
Available online 7 January 2010

Keywords:
Image denoising
Ant colony optimization
Wavelet

ABSTRACT

Wavelet shrinkage is an image denoising technique based on the concept of thresholding the wavelet coefficients. The key challenge of wavelet shrinkage is to find an appropriate threshold value, which is typically controlled by the signal variance. To tackle this challenge, a new image shrinkage approach, called *AntShrink*, is proposed in this paper. The proposed approach exploits the intra-scale dependency of the wavelet coefficients to estimate the signal variance *only* using the homogeneous local neighboring coefficients. This is in contrast to that *all* local neighboring coefficients are used in the conventional shrinkage approaches. Furthermore, to determine the homogeneous local neighboring coefficients, the *ant colony optimization* (ACO) technique is used in this paper to classify the wavelet coefficients. Experimental results are provided to show that the proposed approach outperforms several image denoising approaches developed in the literature.

1. Introduction

Images are often corrupted with noise during image acquisition and image transmission. Wavelet-based algorithms have been proved to be effective for tackling the image denoising problem (Donoho and Johnstone, 1995; Chang et al., 2000; Sendur and Selesnick, 2002; Luisier et al., 2007; Pizurica and Philips, 2006). Motivated by the fact that the wavelet transform packs the energy of the image into a few large coefficients, the simple shrinkage of the coefficients can offer an effective reduction in the corrupting noise. The key challenge is to estimate the signal variance, since it plays a key role to control the degree of shrinkage, consequently controls the quality of the denoised image. The signal variance value is usually estimated based on a local neighborhood of the wavelet coefficient; this local neighborhood could be all of the coefficients in its neighborhood in the same subband (Chang et al., 2000; Sendur and Selesnick, 2002), or the local neighborhood of the wavelet coefficient within the same subband (Eom and Kim, 2004; Mihcak et al., 1999; Shui, 2005).

The estimation of the signal variance from the noisy wavelet coefficients is a critical issue in image shrinkage. Most of the above-mentioned algorithms assume that the wavelet coefficients are locally independent and identically distributed; therefore, the energy distribution of the image in each subband is isotropic. In view of this, they use the isotropic (more specifically, a square-shaped) window for all subbands in each level. However, this is not true for most images, since the signal variances in the wavelet domain exhibit strong intra-scale dependency (Portilla et al., 2003).

To tackle the above challenge, a new image shrinkage approach is proposed in this paper to exploit the intra-scale dependency of the wavelet coefficients for estimating the signal variance *only* using the homogeneous local neighboring coefficients, rather than using *all* local neighboring coefficients in the conventional approaches. To determine the homogeneous local neighboring coefficients, the *ant colony optimization* (ACO) technique is considered as a promising technique to classify the wavelet coefficients in this paper. ACO is a nature-inspired optimization algorithm (Dorigo and Thomas, 2004) motivated by the natural collective behavior of real-world ant colonies. The major collective behavior is the foraging behavior that guides ants on short paths to their food sources, since ants can deposit pheromone on the ground in order to mark some favorable path that should be followed by other members of the colony. Despite that ACO has been widely applied to tackle numerous optimization problems (Dorigo et al., 2000; Cordon et al., 2002; Dorigo et al., 2002), its application in image processing is quite a few (Ouadfel and Batouche, 2003; Hegarat-Mascle et al., 2007; Ghanbarian et al., 2007; Malisia and Tizhoosh, 2006; Tian et al., 2008).

In this paper, the proposed image denoising approach, called *AntShrink*, has two stages, which are sequentially applied for all wavelet coefficients of the noisy image. The first stage of the proposed approach exploits the ACO technique to classify the wavelet coefficients. The second stage of the proposed approach shrinks the

* Corresponding author. Tel./fax: +86 20 87114709.
E-mail addresses: eejtian@gmail.com (J. Tian), yuweiyu@scut.edu.cn (W. Yu), eelhma@scut.edu.cn (L. Ma).

0167-8655/$ - see front matter © 2010 Elsevier B.V. All rights reserved.
doi:10.1016/j.patrec.2010.01.004

noisy wavelet coefficients based on the signal variance that is estimated *only* considering the homogeneous neighboring coefficients, which belong to the same category with that of the central coefficient. Since the neighborhood shape used in the proposed approach automatically adapts to the image segment, the proposed approach has fundamental difference with that the conventional fixed-form neighborhoods (i.e., all neighboring coefficients) considered in the conventional image shrinkage approaches, and the proposed approach is expected to yield superior performance.

The proposed approach yields fundamental difference with the conventional image shrinkage approaches in the following two aspects. First, the proposed approach estimates the signal variance *only* using the homogeneous local neighboring coefficients. On the contrary, the conventional approaches use *all* local neighboring coefficients. Second, to determine the homogeneous local neighboring coefficients, the ACO technique is used in this paper to classify the wavelet coefficients. This is the first time to apply the ACO to tackle the image denoising problem in the wavelet domain, despite its extensive use in various areas in the past.

The rest of this paper is organized as follows. A brief introduction to the ACO technique and the conventional image shrinkage are provided in Section 2 and Section 3, respectively. Then the proposed AnrShrink approach is presented in Section 4, which first exploits the ACO technique to perform image classification and then performs wavelet coefficients shrinkage. Extensive experimental results are provided in Section 5 to compare the proposed approach with a number of image denoising approaches. Finally, Section 6 concludes this paper.

2. Ant colony optimization

In this section, a brief introduction to ACO is proposed. ACO aims to iteratively find the optimal solution of the target problem through a guided search (i.e., the movements of a number of ants) over the solution space, by constructing the *pheromone* information. To be more specific, suppose totally K ants are applied to find the optimal solution in a space χ that consists of $M_1 \times M_2$ nodes, the procedure of ACO can be summarized as follows (Dorigo et al., 2006).

- Initialize the position of each ant, as well as the pheromone matrix $\boldsymbol{\tau}^{(0)}$.
- For the construction-step index $n = 1 : N$,
  - Consecutively move each ant for L steps, according to a probabilistic transition matrix $\mathbf{p}^{(n)}$ (with a size of $M_1M_2 \times M_1M_2$).
  - Update the pheromone information matrix $\boldsymbol{\tau}^{(n)}$.
- Make the solution decision according to the final pheromone information matrix $\boldsymbol{\tau}^{(N)}$.

There are two fundamental issues in the above ACO process; that is, the establishment of the probabilistic transition matrix $\mathbf{p}^{(n)}$ and the update of the pheromone information matrix $\boldsymbol{\tau}^{(n)}$, each of which is presented in detail as follow, respectively.

First, at the nth construction step of ACO, each ant moves from the node i to the node j according to a probabilistic action rule, which is determined by Dorigo et al. (2006)

$$p_{i,j}^{(n)} = \frac{\left(\tau_{i,j}^{(n-1)}\right)^{\alpha}\left(\eta_{i,j}\right)^{\beta}}{\sum_{j\in\Omega_i}\left(\tau_{i,j}^{(n-1)}\right)^{\alpha}\left(\eta_{i,j}\right)^{\beta}}, \tag{1}$$

where $\tau_{i,j}^{(n-1)}$ is the pheromone information value of the arc linking the node i to the node j; Ω_i is the neighborhood nodes for the ant a_k given that it is on the node i; the constants α and β represent the influence of the pheromone information and the heuristic information, respectively; $\eta_{i,j}$ represents the heuristic information for going from node i to node j, which is fixed to be same for each construction step.

Second, the pheromone information matrix needs to be updated twice during the ACO procedure. The first update is performed after the movement of each ant within each construction step. More specifically, after the movement of each ant within the nth construction step, the pheromone information matrix is updated as (Dorigo et al., 2006)

$$\tau_{i,j}^{(n-1)} = \begin{cases} \tau_{i,j}^{(n-1)} + \Delta_{i,j}^{(k)}, & \text{if } (i,j) \text{ belongs to the } \textit{best tour}; \\ \tau_{i,j}^{(n-1)}, & \text{otherwise}. \end{cases} \tag{2}$$

Furthermore, the determination of *best tour* is subject to the user-defined criterion, it could be either the best tour found in the current construction step, or the best solution found since the start of the algorithm, or a combination of both of the above two (Dorigo et al., 2006). The second update is performed after the move of *all K* ants within each construction step; and the pheromone information matrix is updated as (Dorigo et al., 2006)

$$\boldsymbol{\tau}^{(n)} = (1-\psi)\cdot\boldsymbol{\tau}^{(n-1)} + \psi\cdot\boldsymbol{\tau}^{(0)}, \tag{3}$$

where ψ is the *pheromone decay coefficient*.

3. Conventional image shrinkage approach

A noisy image in wavelet domain can be mathematically modeled as (Mihcak et al., 1999)

$$\mathbf{y} = \mathbf{s} + \mathbf{n}, \tag{4}$$

where $\mathbf{y}$ is the observed noisy coefficients, $\mathbf{s}$ is the unknown original (noise-free) coefficients, and $\mathbf{n}$ is assumed to be a white Gaussian noise with a zero mean and a variance σ_n^2. The goal of image deno-

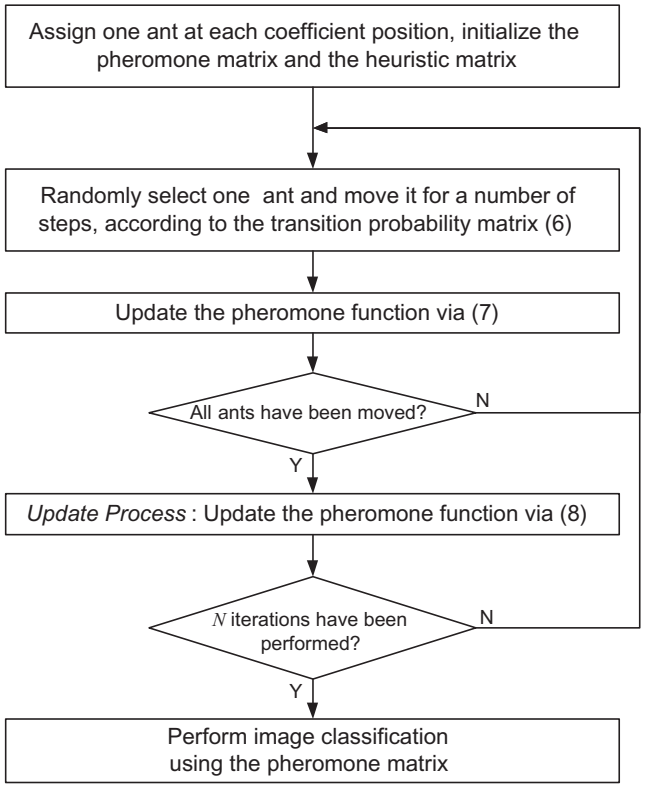

Fig. 1. A summary of the implementation of the proposed ACO-based image classification approach.

ising is to recover the signal **s** from the noisy observation **y**. Given the signal variance σ_i^2 for a wavelet coefficient s_i, which is assumed to be an independent Gaussian variable, the *minimum mean square error* (MMSE) estimator of s_i is given by Mihcak et al. (1999).

$$\hat{s}_i = \frac{\sigma_i^2}{\sigma_i^2 + \sigma_n^2} y_i. \tag{5}$$

The key issue of the above method is to estimate the signal variance (i.e., σ_i^2 in (5)). Non-exact estimation of signal values would result in non-exact estimation of the denoised signal value; consequently, the denoised image would suffer from non-satisfied perceptual visual quality. More specifically, for the coefficients that have a large signal content, that is, $\sigma_i^2 \gg \sigma_n^2$; this results in a negligible shrinkage of these coefficients. On the other hand, for a noise-dominated coefficient, that is, $\sigma_i^2 \ll \sigma_n^2$; that results in a large shrinkage of the corresponding coefficient.

4. AntShrink: the proposed image denoising approach

In view of estimating the signal variance is a key challenge of image shrinkage, an AntShrink approach is proposed in this section to exploit the intra-scale dependency of the wavelet coefficients for estimating the signal variance *only* using the homogeneous neighboring coefficients, rather than using *all* neighboring coefficients in the conventional approaches. The proposed AntShrink approach has two stages: (i) exploit the ACO technique to classify the wavelet coefficients; and (ii) shrink the noisy wavelet coefficient according to a locally-adapted signal variance value. To be more specific, for each coefficient position, the signal variance value is estimated using the neighboring coefficients yielding the same category (as determined by the proposed ACO-based classification method) as that of the center coefficient under consideration. This is in contrast to the conventional image shrinkage approaches that use *all* neighboring coefficients. Both of these two stages are presented in detail in the following.

4.1. First stage—classify wavelet coefficients using the ACO technique

The proposed ACO-based image classification approach aims to utilize a number of ants to move on a 2-D image for constructing a pheromone matrix, each entry of which represents certain feature at each pixel location of the image. Furthermore, the movements of the ants are steered by the amplitude information of the wavelet coefficient.

The proposed approach starts from assigning one ant on an image with a size of $M_1 \times M_2$, each pixel of which can be viewed as a node. Furthermore, the initial value of each component of the pheromone matrix $\tau^{(0)}$ is set to be a constant τ_{init}. Then the proposed algorithm runs for N iterations, in each iteration, each ant moves to neighboring coefficients and the pheromone content of the coefficient on the ant's path are updated. Finally, an image classification is performed at each wavelet coefficient by considering the normalized pheromone matrix using the K-means clustering algorithm, where $K = 2$ in our context.

4.1.1. Ant movement

At the nth iteration, one ant is randomly selected, and this ant will consecutively move on the image for L steps. This ant moves from the node (l,m) to its neighboring node (i,j) according to a transition probability that is defined as

$$p_{(l,m),(i,j)}^{(n)} = \frac{\left(\tau_{i,j}^{(n-1)}\right)^{\alpha}\left(\eta_{i,j}\right)^{\beta}}{\sum_{(i,j)\in\Omega_{(l,m)}}\left(\tau_{i,j}^{(n-1)}\right)^{\alpha}\left(\eta_{i,j}\right)^{\beta}}, \tag{6}$$

where $\tau_{i,j}^{(n-1)}$ is the pheromone value of the node (i,j), $\Omega_{(l,m)}$ is the neighborhood nodes of the node (l,m), $\eta_{i,j}$ represents the heuristic information at the node (i,j). The constants α and β represent the influence of the pheromone matrix and the heuristic matrix, respectively.

There are two crucial issues in the construction process. The first issue is the determination of the heuristic information $\eta_{i,j}$ in (6). In this paper, it is proposed to be determined by the local statistics at

Table 1
The PSNR performance comparison.

Algorithm	Additive white Gaussian noise			
	$\sigma_n = 10$	$\sigma_n = 15$	$\sigma_n = 20$	$\sigma_n = 25$
Test image Barbara				
SureShrink (Donoho and Johnstone, 1995)	30.98	28.69	27.10	26.01
OracleShrink (Chang et al., 2000)	31.26	28.84	27.19	26.06
BayesShrink (Chang et al., 2000)	30.85	28.48	27.02	25.98
BiShrink (Sendur and Selesnick, 2002)	32.06	29.76	28.09	26.94
SURELet (Luisier et al., 2007)	31.54	29.30	27.72	26.60
ProbShrink (Pizurica and Philips, 2006)	31.47	29.02	27.64	26.61
Proposed *AntShrink*	32.55	30.31	28.65	27.47
Test image Boat				
SureShrink (Donoho and Johnstone, 1995)	31.81	29.80	28.46	27.46
OracleShrink (Chang et al., 2000)	31.94	29.87	28.50	27.48
BayesShrink (Chang et al., 2000)	31.71	29.77	28.41	27.39
BiShrink (Sendur and Selesnick, 2002)	32.25	30.35	29.01	27.99
SURELet (Luisier et al., 2007)	32.30	30.36	29.07	28.04
ProbShrink (Pizurica and Philips, 2006)	31.65	30.03	28.70	27.70
Proposed *AntShrink*	32.66	30.70	29.26	28.14
Test image Window				
SureShrink (Donoho and Johnstone, 1995)	30.35	27.78	26.09	24.87
OracleShrink (Chang et al., 2000)	30.46	27.83	26.11	24.89
BayesShrink (Chang et al., 2000)	30.30	27.77	26.07	24.83
BiShrink (Sendur and Selesnick, 2002)	30.80	28.27	26.57	25.34
SURELet (Luisier et al., 2007)	30.58	28.18	26.55	25.38
ProbShrink (Pizurica and Philips, 2006)	29.92	27.92	26.25	25.03
Proposed *AntShrink*	31.21	28.71	27.03	25.80

the pixel position (i,j) as the inverse of the absolute value of the difference between the wavelet coefficient (i,j) and the mean of the current path. The second issue is to determine the permissable range of the ant's movement (i.e., $\Omega_{(l,m)}$ in (6)) at the position (l,m). In this paper, it is proposed to be 8-connectivity neighborhood.

4.1.2. Pheromone update

The proposed approach performs two updates operations for updating the pheromone matrix.

- The first update is performed after the movement of each ant within each construction-step. Each component of the pheromone matrix is updated according to

$$\tau_{i,j}^{(n-1)} = \begin{cases} (1-\rho)\cdot\tau_{i,j}^{(n-1)} + \rho\cdot\Delta_{i,j}^{(k)}, & \text{if } (i,j) \text{ is visited by the current } k\text{th ant;} \\ \tau_{i,j}^{(n-1)}, & \text{otherwise.} \end{cases} \tag{7}$$

where ρ is defined in (2), $\Delta_{i,j}^{(k)}$ is determined by the heuristic matrix; that is, $\Delta_{i,j}^{(k)} = \frac{1}{|\eta_{i,j}|}$.

- The second update is carried out after the movement of all ants within each construction-step according to

$$\boldsymbol{\tau}^{(n)} = (1-\psi)\cdot\boldsymbol{\tau}^{(n-1)} + \psi\cdot\boldsymbol{\tau}^{(0)}, \tag{8}$$

where ψ is defined in (3).

4.1.3. Summary of the first stage

A summary of the implementation of the proposed approach is presented in Fig. 1. The proposed approach starts from the initial-

Fig. 2. Various results of *Barbara*: (a) ground truth; (b) noisy image that is generated by adding a white Gaussian noise (a zero mean and a standard deviation $\sigma_n = 15$) to the image (a); (c) *SureShrink* (Donoho and Johnstone, 1995) (PSNR = 28.69 dB); (d) *OracleShrink* (Chang et al., 2000) (PSNR = 28.84 dB); (e) *BayesShrink* (Chang et al., 2000) (PSNR = 28.48 dB); (f) *BiShrink* (Sendur and Selesnick, 2002) (PSNR = 29.76 dB); (g) *SURELet* (Luisier et al., 2007) (PSNR = 29.30 dB); (h) *ProbShrink* (Pizurica and Philips, 2006) (PSNR = 29.02 dB); and (i) our proposed *AntShrink* approach (PSNR = 30.31 dB).

ization process, and then runs for N iterations to construct the pheromone matrix by performing both the construction process and the update process. Finally, the category of each wavelet coefficient is determined according to the above-constructed pheromone matrix.

4.2. Second stage—shrinkage

The proposed method first estimates each signal variance based on its homogeneous neighboring coefficients, which belong to the same category with that of the central coefficient, and finally incorporates the estimated variance values into the conventional MMSE estimator (5) to obtain the denoised signal. More specifically, the proposed approach is summarized as follows.

- Perform a 2-D discrete wavelet decomposition on a noisy image to get the noisy wavelet coefficients.
- Perform the ACO-based classification using the method presented in Section 4.1.
- Estimate the signal variance $\hat{\sigma}_i^2$ for each coefficient excluding those of the *LL* subband via

$$\hat{\sigma}_i^2 = \left(\frac{1}{|c(i)|} \sum_{y_j \in c(y_i)} y_j^2 - \hat{\sigma}_n^2 \right)_+, \tag{9}$$

  where $c(y_i)$ is defined as the coefficients within a local square window and *have the same category* as that is centered at the coefficient y_i, and $|c(y_i)|$ is the cardinality (i.e., the number of coefficients) of $c(y_i)$, the output of the function $(x)_+$ is 1, if $x > 0$; otherwise, the output is 0. Note that the proposed approach differs with the conventional image shrinkage methods, where *all* local neighboring coefficients are used in $c(y_i)$. Furthermore, the noise variance σ_n^2 is estimated via $\hat{\sigma}_n = median|y_i|/0.6745$ (Donoho and Johnstone, 1995), where the coefficient y_i belongs to the highest HH subband.
- Compute the MMSE estimation for each coefficient excluding those of the *LL* subband, by substituting the noise variance estimated via (9) into (5).

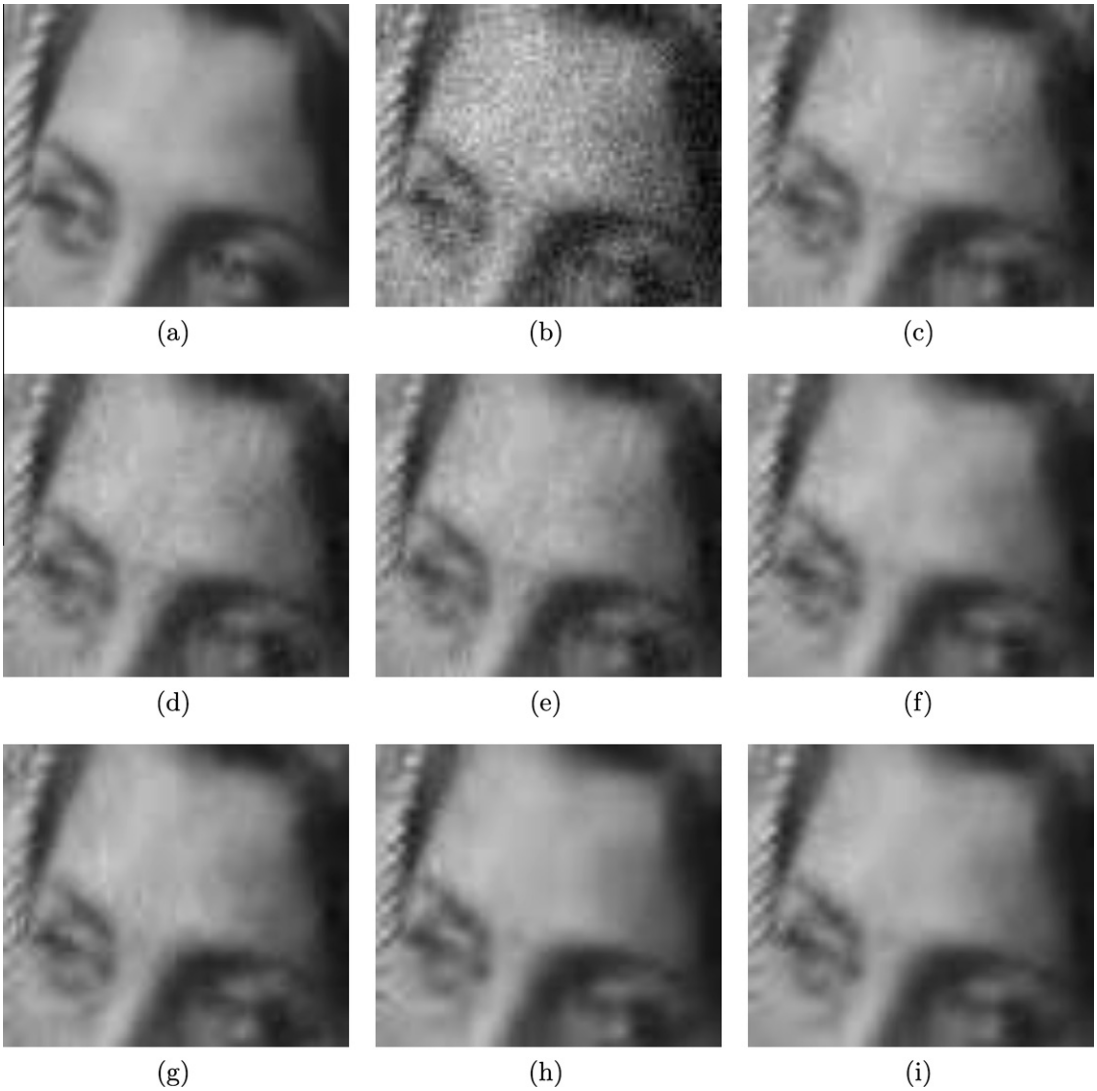

Fig. 3. Various parts of the results of *Barbara*; which are the corresponding parts of images presented in Fig. 2: (a) ground truth; (b) noisy image that is generated by adding a white Gaussian noise (a zero mean and a standard deviation $\sigma_n = 15$) to the image (a); (c) *SureShrink* (Donoho and Johnstone, 1995) (PSNR = 28.69 dB); (d) *OracleShrink* (Chang et al., 2000) (PSNR = 28.84 dB); (e) *BayesShrink* (Chang et al., 2000) (PSNR = 28.48 dB); (f) *BiShrink* (Sendur and Selesnick, 2002) (PSNR = 29.76 dB); (g) *SURELet* (Luisier et al., 2007) (PSNR = 29.30 dB); (h) *ProbShrink* (Pizurica and Philips, 2006) (PSNR = 29.03 dB); and (i) our proposed *AntShrink* approach (PSNR = 30.31 dB).

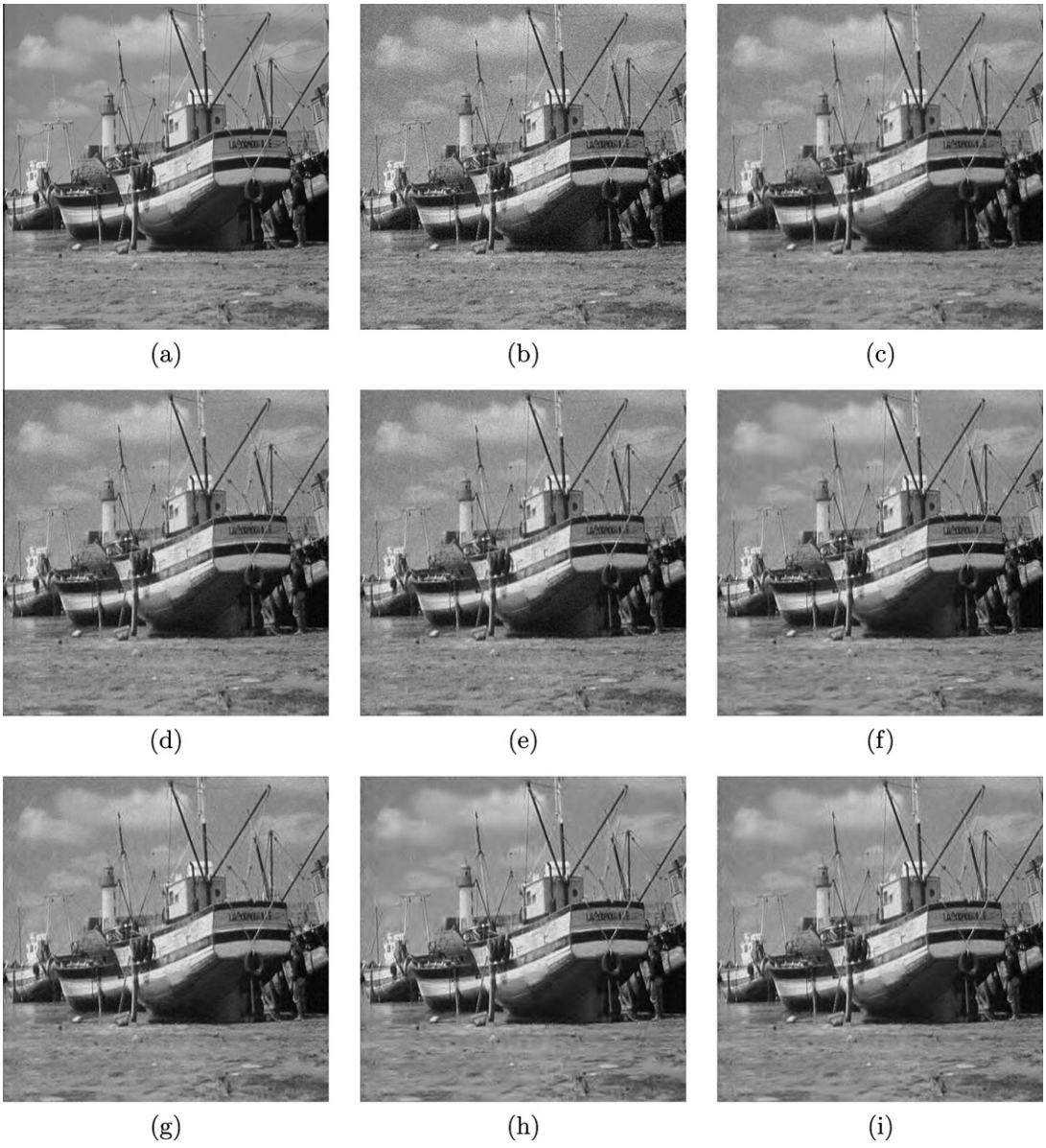

Fig. 4. Various results of *Boat*: (a) ground truth; (b) noisy image that is generated by adding a white Gaussian noise (a zero mean and a standard deviation $\sigma_n = 15$) to the image (a); (c) *SureShrink* (Donoho and Johnstone, 1995) (PSNR = 29.80 dB); (d) *OracleShrink* (Chang et al., 2000) (PSNR = 29.87 dB); (e) *BayesShrink* (Chang et al., 2000) (PSNR = 29.77 dB); (f) *BiShrink* (Sendur and Selesnick, 2002) (PSNR = 30.35 dB); (g) *SURELet* (Luisier et al., 2007) (PSNR = 30.36 dB); (h) *ProbShrink* (Pizurica and Philips, 2006) (PSNR = 30.03 dB); and (i) our proposed *AntShrink* approach (PSNR = 30.70 dB).

- Finally, perform the inverse wavelet transform to obtain the denoised image.

5. Experimental results

Experiments are conducted to explore the performance of the proposed method using the well-known test images 512×512 *Barbara*, 512×512 *Boat* and 512×512 *Window*, which serve as the ground truth and compared with the denoised images for performance comparison, respectively. The noisy images are generated by adding the ground truth image with an additive white Gaussian noise with a zero mean and a standard deviation σ_n, respectively. The wavelet decomposition is implemented via a five-level decomposition using a *Daubechies*'s wavelet with eight vanishing moments. The window size used in (9) for estimating the signal variance is set to be 5×5. Furthermore, the parameters of the proposed ACO-based classification approach are experimentally set as follows: $\tau_{init} = 0.0001$, $\alpha = 1$, $\beta = 2$, $L = 15$, and $\psi = 0.3$.

The first experiment is to compare the proposed method with other six denoising methods; they are *SureShrink* (Donoho and Johnstone, 1995), *OracleShrink* (Chang et al., 2000), *BayesShrink* (Chang et al., 2000), *BiShrink* (Sendur and Selesnick, 2002), *SURELet* (Luisier et al., 2007), and *ProbShrink* (Pizurica and Philips, 2006). Table 1 compares the PSNR performances of the above mentioned methods, where the output PSNRs have been averaged over ten noise realizations. Figs. 2–5 provide the subjective performance comparison. As seen from the above table and figures, the proposed algorithm always outperforms the above six denoising methods to yield the best objective performance as well as the best subjective performance.

The second experiment is to explore the computational complexity of the proposed approach. The above denoising approaches are implemented using the *Matlab* programming language and run

Fig. 5. Various results of *Window*: (a) ground truth; (b) noisy image that is generated by adding a white Gaussian noise (a zero mean and a standard deviation $\sigma_n = 15$) to the image (a); (c) *SureShrink* (Donoho and Johnstone, 1995) (PSNR = 27.78 dB); (d) *OracleShrink* (Chang et al., 2000) (PSNR = 27.83 dB); (e) *BayesShrink* (Chang et al., 2000) (PSNR = 27.77 dB); (f) *BiShrink* (Sendur and Selesnick, 2002) (PSNR = 28.27 dB); (g) *SURELet* (Luisier et al., 2007) (PSNR = 28.18 dB); (h) *ProbShrink* (Pizurica and Philips, 2006) (PSNR = 27.92 dB); and (i) our proposed *AntShrink* approach (PSNR = 28.71 dB).

on a PC with a Pentium 2.6 GHz CPU and a 4096 MB RAM. One hundred experiments are conducted for each of the above-mentioned approaches. Furthermore, the computational complexity (in terms of the run time) of the proposed approach is compared with that of the above six denoising approaches, and their respective average run-times are presented in Table 2.

Table 2
The run-time comparison (in seconds).

Algorithm	Run time
SureShrink (Donoho and Johnstone, 1995)	0.93
OracleShrink (Chang et al., 2000)	1.14
BayesShrink (Chang et al., 2000)	0.87
BiShrink (Sendur and Selesnick, 2002)	0.91
SURELet (Luisier et al., 2007)	1.13
ProbShrink (Pizurica and Philips, 2006)	1.16
Proposed *AntShrink*	28.50

6. Conclusions

An AntShrink approach has been proposed in this paper to perform image denoising. The proposed approach exploits the ACO technique to classify the wavelet coefficients for constructing the neighborhood shape that automatically adapts to the image segment (i.e., the neighboring coefficients belonging to the same category with that of the central coefficient). This has been shown to be superior to the conventional fixed-form neighborhoods (i.e., all neighboring coefficients) considered in the conventional image shrinkage approaches, as verified in our experiments.

There are several directions could be considered for future research. First, the proposed approach is independently applied for each high-pass filtered subband of the noisy image. It could be further improved by considering the inter-scale correlation among the wavelet coefficients (Sendur and Selesnick, 2002) to perform classifying. Second, the parallel ACO algorithm (Randall and Lewis,

2002) can be exploited to further reduce the computational load of the proposed image classification algorithm; consequently, shorten the execution time of the proposed approach.

Acknowledgements

The authors thank the authors of Donoho and Johnstone (1995); Chang et al. (2000); Sendur and Selesnick (2002); Luisier et al. (2007); Pizurica and Philips (2006) for providing their respective image denoising programs available online. This work was supported by National Natural Science Foundation of China (Grant No. 60972133) and Guangdong Science Fund (Grant No. 9351064101000003), the National Natural Science Foundation of China (Grant No. 60872123), the Joint Fund of the National Natural Science Foundation and the Guangdong Provincial Natural Science Foundation (Grant No. U0835001), the Fund of Provincial Key Laboratory for Computer Information Processing Technology, Suzhou, (Grant No. KJS0922).

References

Chang, S.G., Yu, B., Vetterli, M., 2000. Spatially adaptive wavelet thresholding with context modeling for image denoising. IEEE Trans. Image Process. 9, 1522–1531.
Cordon, O., Herrera, F., Stutzle, T., 2002. Special issue on ant colony optimization: models and applications. Mathware and Soft Computing 9.
Donoho, D.L., Johnstone, I.M., 1995. Adapting to unknown smoothness via wavelet shrinkage. J. Am. Statist. Assoc. 90, 1200–1224.
Dorigo, M., Thomas, S., 2004. Ant Colony Optimization. MIT Press, Cambridge.
Dorigo, M., Caro, G.D., Stutzle, T., 2000. Special issue on ant algorithms. Future Generation Computer Systems 16.
Dorigo, M., Gambardella, L.M., Middendorf, M., Stutzle, T., 2002. Special issue on ant colony optimization. IEEE Trans. Evolution. Comput. 6.
Dorigo, M., Birattari, M., Stutzle, T., 2006. Ant colony optimization. IEEE Comput. Intell. Mag. 1, 28–39.
Eom, I.K., Kim, Y.S., 2004. Wavelet-based denoising with nearly arbitrarily shaped windows. IEEE Signal Process. Lett. 11, 937–940.
Ghanbarian, A.T., Kabir, E., Charkari, N.M., 2007. Color reduction based on ant colony. Pattern Recognition Lett. 28, 1383–1390.
Hegarat-Mascle, S.L., Kallel, A., Descombes, X., 2007. Ant colony optimization for image regularization based on a nonstationary Markov modeling. IEEE Trans. Image Process. 16, 865–878.
Luisier, F., Blu, T., Unser, M., 2007. A new SURE approach to image denoising: interscale orthonormal wavelet thresholding. IEEE Trans. Image Process. 16, 593–606.
Malisia, A.R., Tizhoosh, H.R., 2006. Image thresholding using ant colony optimization. In: Proc. Canadian Conf. on Computer and Robot Vision, Quebec, Canada, pp. 26–26.
Mihcak, M.K., Kozintsev, I., Ramchandran, K., Moulin, P., 1999. Low-complexity image denoising based on statistical modeling of wavelet coefficients. IEEE Signal Process. Lett. 6, 300–303.
Ouadfel, S., Batouche, M., 2003. Ant colony system with local search for Markov random field image segmentation. In: Proc. IEEE Internat. Conf. on Image Processing, Barcelona, Spain, pp. 133–136.
Pizurica, A., Philips, W., 2006. Estimating the probability of the presence of a signal of interest in multiresolution single- and multiband image denoising. IEEE Trans. Image Process. 15, 654–665.
Portilla, J., Strela, V., Wainwright, M.J., Simoncelli, E.P., 2003. Image denoising using scale mixtures of Gaussians in the wavelet domain. IEEE Trans. Image Process. 12, 1338–1351.
Randall, M., Lewis, A., 2002. A parallel implementation of ant colony optimization. J. Parallel Distributed Comput. 62, 1421–1432.
Sendur, L., Selesnick, I.W., 2002. Bivariate shrinkage with local variance estimation. IEEE Signal Process. Lett. 9, 438–441.
Shui, P.-L., 2005. Image denoising algorithm via doubly local wiener filtering with directional windows in wavelet domain. IEEE Signal Process. Lett. 12, 681–684.
Tian, J., Yu, W., Xie, S., 2008. An ant colony optimization algorithm for image edge detection. In: Proc. IEEE Congress on Evolutionary Computation, Hongkong, China, pp. 751–756.